

**Segregation and intermixing in polydisperse liquid-solid fluidized beds: A multifluid
model validation study**

Shashank S. Tiwari^{1,2}, Swapnil V. Ghatage³, Jyeshtharaj B. Joshi^{2,4*}, Bo Kong^{1*}

¹ Department of Chemical Engineering, Guangdong Technion-Israel Institute of Technology,
Shantou, Guangdong, 515063, China

² Department of Chemical Engineering, Institute of Chemical Technology, Matunga,
Mumbai-400019, India.

³ D Engineering Automation LLP, Pune, 411021, India

⁴ Homi Bhabha National Institute, Anushaktinagar, Mumbai-400094, India

* Author to whom correspondence may be addressed.

Phone: +91-22-25597625, Fax: +91-22-33611020, E-mail: jb.joshi@ictmumbai.edu.in,

bo.kong@gtiit.edu.cn

ABSTRACT

Multifluid model (MFM) simulations have been carried out on liquid-solid fluidized beds (LSFB) consisting of binary and higher-order polydisperse particle mixtures. The role of particle-particle interactions was found to be as crucial as the drag force under laminar and homogenous LSFB flow regimes. The commonly used particle-particle closure models are designed for turbulent and heterogeneous gas-solid flow regimes and thus exhibit limited to no success when implemented for LSFB operating under laminar and homogenous conditions. A need is perceived to carry out Direct Numerical Simulations of liquid-solid flows and extract data from them to develop rational closure terms to account for the physics of LSFB. Finally, a recommendation flow regime map signifying the performance of the MFM has been proposed. This map will act as a potential guideline to identify whether or not the bed expansion characteristics of a given polydisperse LSFB can be correctly simulated using MFM closures tested.

Keywords: Polydisperse liquid-solid flow; fluidized bed, segregation and intermixing; Euler-Euler simulations; Computational Fluid Dynamics

1 INTRODUCTION

Liquid-solid fluidized beds (LSFB) are widely used in the chemical and petrochemical industries. LSFB finds its application in several unit processes: roasting of ores, effluent treatment, chromatographic separations, and crystallization. For most of these processes, the LSFB operates with a mixture of different particles with wide size, shape, density distribution, and phase volume fractions. A wide range of settling velocities characterizes these particles. While designing LSFB, it is essential to understand the bed expansion, particle segregation, and intermixing of various solid phases. One of the critical parameters affecting the performance of LSFB is the operating conditions such as particle size distribution and solid loading. These characteristics govern the equipment volume depending upon the phase in

which the various sub-processes take place. Further, the spatial distribution of solid phase volume fraction governs the flow pattern of solid and liquid phases. It thus indirectly affects the extent of liquid and solid phase mixing, axial dispersion in both the phases, mass, heat, momentum transfer and chemical reaction rates.

The modeling of such systems offers challenges because of the complexity of flow and interfacial forces involved. Computational fluid dynamics (CFD) is a powerful tool to predict the flow and bed expansion characteristics accurately. Various researchers successfully employed the Eulerian-Eulerian (E-E) framework-based multifluid model (MFM) to predict expansion characteristics in mono-component LSF_B¹⁻⁴ and segregation and intermixing behavior in binary LSF_B⁵⁻⁸. The MFM approach considers interpenetrating continua of phases and involves the kinetic theory of granular flow (KTGF) as closure. Due to the assumption of interpenetrating continua, the MFM approach possesses an inherent limitation of modeling the interfacial interaction terms. Most of the commonly used interfacial interaction models used to provide closures are based on empirical or semi-empirical models, which makes their use restricted under specific flow conditions. The limitations posed by the MFM can be overcome by using a more rational approach such as (i) the Computational Fluid Dynamics-Discrete Element Method (CFD-DEM) approach, which solves the equation of motion tracking the trajectory of each particle, thereby considering them as discrete entities^{9,10}. (ii) Direct Numerical Simulations (DNS) – solving the fundamental governing equations for the continuous and the dispersed phases without averaging or filtering approaches. Although both CFD-DEM and DNS provide a much rational solution, they are computationally intensive and expensive for simulating polydisperse LSF_B. The application of such high fidelity approaches (CFD-DEM and DNS) is limited to a few particles for a reduced order geometry or under simplified assumptions^{11,12}. On the other hand, the relatively simple physics of the interpenetrating continuum provided by the MFM approach makes it convenient and

economically feasible to investigate the overall performance of industrial-scale LSF. Thus, although the predictions from the Eulerian-Eulerian approach are not as informative and accurate as DNS or the CFD-DEM, the possibility of getting quick estimates for design parameters of industrial-scale equipment makes them essential. The present work uses the MFM approach to study the bed expansion, segregation, and intermixing in LSF involving different particle phases (2 to 6 species). The current information from the literature on segregation and intermixing in LSF have been first systematically reviewed and discussed in the following sub-section. The lacune identified from this literature review has been then presented at the end of this section.

1.1 Literature review

The parameters affecting the segregation and intermixing behavior in LSF include particle size, particle shape, phase densities, volume fraction, and liquid-phase velocity (the present study only focuses on polydispersity due to particle size and density). Researchers have proposed correlations for segregation based on these parameters. Fluidization of particles leads to bed expansion, whose height changes with the fluid flow rate. The expansion characteristics of mono-disperse LSF have been well represented empirically by the Richardson and Zaki¹³ equation (1):

$$\frac{V_L}{V_{s\infty}} = \epsilon_L^n \quad (1)$$

Here n is an empirical parameter and can be estimated using Richardson and Zaki¹³, V_L is the superficial liquid velocity, and $V_{s\infty}$ is the terminal settling velocity for a single particle. When a second solid component that differs either in size or density or in both is introduced, the bed expansion characteristics get more complicated. The two species of solid particles have different settling velocities, the difference in which causes the particles to either segregate or intermix. The height of the intermixing zone depends upon the ratio of terminal settling

velocities ($V_{S1\infty}/V_{S2\infty}$) and the Reynolds number. In extreme cases, the binary particles segregate with a clear interface or intermix entirely so that both the particles are found everywhere in the expanded bed. The prediction of segregation and intermixing effects becomes more complex as the number of particle phases increases.

1.1.1 Experimental studies

Hoffman et al.¹⁴ experimentally observed that such behavior depends on the size ratio in binary and ternary particle systems having the same density. They observed complete segregation when the size ratio of the larger particle to the smaller particle ($d_R = d_{S_1}/d_{S_2}$) was greater than 1.58 and partial segregation when the size ratio was 1.24. Pruden and Epstein¹⁵ proposed that the degree of segregation depends on the difference between the bulk densities of two solid species when each species is fluidized individually. It was found that the higher the value of bulk density difference, the greater is the tendency towards segregation. The value of bulk density difference increases with an increase in the size ratio (d_R) and liquid voidage (ϵ_L).

Wen and Yu¹⁶ carried out experiments for bidisperse size for particles having the same density. They found that for $d_R < 1.3$, the particles intermix while for $d_R > 1.3$, they segregate. Al-Dibouni and Garside¹⁷ investigated bidisperse LSF in the range of size ratios $2 < d_R < 6.7$. They found that particle combinations having $d_R \geq 2.1$, exhibit complete segregation. Galvin et al.¹⁸ carried out experiments for LSF with a binary particle system where the two-particle species varied mainly in density ($1.06 < \rho_{S_1}/\rho_{S_2} < 1.18$). The particle sizes of each of the selected solid species ranged from $1\text{mm} < d_{S_i} < 1.18\text{mm}$. Their experiments showed that the closer the terminal settling velocity of the particle species in a given binary LSF, the greater will be the intermixing between them. Galvin et al.¹⁸ also developed a one-dimensional algebraic model to predict the axial varying solid hold-up and the dispersion coefficient for

binary LSFb. It is worth noting that all of the previously existing models (before Galvin et al.¹⁸) assumed that the solid dispersion coefficient remains uniform throughout the bed. The model proposed by Galvin et al.¹⁸ showed that the solid dispersion coefficient depends upon the local condition and thereby varies along with the axial distance of the LSFb.

Murli et al.¹⁹ carried out experiments for six different sizes of particles (constant particle density for all size sizes). They used the experimental data to propose a simplified correlation for estimating the overall solid dispersion coefficient using the equivalent diameter and minimum fluidization velocity for the system under study. They found that the solid dispersion coefficient increases with an increase in particle diameter and superficial liquid velocity. The work of Murli et al.¹⁹ was taken forward by Chavan and Joshi²⁰, who experimentally investigated binary and higher polydispersity LSFb (3 to 5 sizes of particles having the same particle density). Their experiments led to the finding that the segregation of a given particle species in a polydisperse LSFb is a strong function of the size ratio of that particle species to the other particle species present in the bed. They used the correlation for reduced bulk density (β) proposed by Epstein and Pruden¹⁵ in combination with their experimental results to show that for a binary LSFb, complete segregation takes place for $d_r \geq 1.55$, partial segregation occurs for $1.4 \leq d_r < 1.55$, and complete intermixing happens for $d_r \leq 1.4$.

In higher polydispersity LSFb, with each new particle-phase added, it was observed that the intermixing effects become more dominant, and complete segregation was no longer observed up to a particle size ratio equal to 2. In LSFb with the ternary mixture, partial intermixing was observed for a size ratio of 1.4, whereas relatively less intermixing was seen for a size ratio of 1.7. For a ternary particle mixture of an equal diameter ratio of 1.41, equal distribution of mid-sized particles was observed between the large and small particle sizes. The ternary mixture experiments were found to attain a steady-state condition after 2hrs. After the steady-state was reached, the largest size particles (out of the three particle sizes that were fluidized) settled

down at the bottom of the bed. The mid-sized particles settled above the large ones while the smallest ones were amassed at the top.

Chavan and Joshi²⁰ showed that intermixing effects were predominant over segregation effects and particles in the mixed zones in the bed in fluidized bed systems involving four different particle sizes. The maximum extent of intermixing impact was seen for particles of the smallest size ratios. In five particle systems, an increased extent of intermixing was observed compared to that in the quaternary system. However, the layers of the smallest and largest particles sizes still existed at the top and the bottom regions of the bed. A small intermixed zone was present in between where particles of all the five different sizes were present.

Khan et al.⁷ showed that the bed expansion heights of each solid phase of a completely segregated binary LSFBS deviate by around 23-25% than the corresponding bed expansion heights exhibited by monosized LSFBS. Binary LSFBS with high particle density ratios, even when showing dominant segregation, were found to have a small mixing zone which decreased as the superficial liquid velocity increased. In contrast, small diameter ratio cases illustrated a comparatively larger mixing zone, which increased with superficial fluid velocity.

1.1.2 Computational Studies

In addition to the theoretical models and experimental studies, the last two decades have seen a tremendous increase in computational studies of segregation and intermixing characteristics in binary LSFBS. Chen et al.²¹ developed a simplified one-dimensional hydrodynamic model for predicting the solid hold-up in the LSFBS. They used the drag correlation of Clift et al.²² in their hydrodynamic model. They found that the solid phase axial hold-up predicted by their model agreed well with experimental data for mono, binary and multi-size particle systems for high fluidization velocities. However, their model did predict segregation for low fluidization velocities where segregation is not observed in experiments. They also showed that a binary mixture (with both particles having the same particle density) would segregate itself into two

separate layers if the superficial liquid velocity of the LSFBS lies between the individual minimum fluidization velocity of each of the particle phases. Gera et al.²³ studied particle segregation in a binary gas-solid fluidized bed using the Eulerian-Eulerian model. They used the Gidaspow²⁴ model to account for the fluid-solid interaction. In addition to the fluid-solid drag, they proposed a new term to account for interactions between solids that they call particle-to-particle drag. They found that the inclusion of the particle-particle drag accurately models the hindrance effect, which correctly predicts the segregation at intermixing behavior. Reddy and Joshi⁶ performed E-E framework-based MFM simulations for mono and binary particle mixture LSFBS covering a wide range of particle size ratios. Their simulations were found to be in good agreement with the experimentally predicted solid hold-ups, provided the Pandit and Joshi²⁵ fluid-particle drag model was used.

Jain et al.²⁶ investigated the flow behavior in a binary LSFBS using Radioactive Particle Tracking (RPT) and Dense Discrete Particle Method (DDPM). The mean velocity predictions of DDPM were found to be in good agreement with the experimental measurements. However, the axial root mean square (RMS) velocity predictions were reasonably predicted by DDPM only for bigger (1mm) particles. The deviation in RMS velocity predictions from DDPM occurred due to the limitations in quantifying the particle-particle interactions.

Khan et al.⁸ carried out two-dimensional MFM simulations for binary LSFBS using the kinetic theory of granular flow (KTGF). The predicted axial profiles from the simulation were found to be in good agreement with the experimental data from published literature. It was found that binary mixtures exhibit complete/partial intermixing. The energy dissipation rate significantly increased with the superficial liquid velocity indicating the presence of strong phase interactions.

Peng et al.²⁷ carried out computational fluid dynamics-discrete element model (CFD-DEM) simulations of binary particle mixture in LSFBS to evaluate the interfacial forces acting under

various flow regimes. It was found that under heterogeneous flow conditions ($Re_p > 40$, $\varepsilon_{L,avg} > 0.74$), the local fluid-phase turbulence governs the axial and radial dispersion of particle phases. In contrast, for the homogenous flow regime ($Re_p \leq 40$, $\varepsilon_{L,avg} \leq 0.74$), the binary LSFB hydrodynamics strongly depends on the particle-particle collisions.

Rahaman et al.²⁸ carried out MFM simulations in six-size polydisperse LSFB to investigate the flow patterns. Their simulations were limited to particle systems which show dominant segregation of particles. They evaluated three empirical fluid-solid drag laws to understand the rate of fluid-solid momentum transfer. Wen and Yu¹⁶ and Gidaspow²⁴ drag law models showed better hydrodynamics predictions as compared to the Syamlal²⁹ model.

Molaei et al.³⁰ used the CFD-DEM to investigate the segregation in binary particle mixture LSFB. They found that the fluid-particle drag plays an essential role in imparting segregation to a given particle mixture. They found that the conventional drag laws based on monosized particle mixtures may not accurately predict the accurate flow patterns of particle mixtures consisting of different sizes and densities, as was earlier argued by Di-Renzo et al.³¹. Molaei et al.³⁰ used drag models designed specifically for polydisperse particle mixtures to provide closure for the fluid-particle momentum transfer. They found that the segregation behavior is best predicted when the drag model of Rong et al.³² is used.

Previously reported segregation and intermixing studies have been carried out over a wide range of flow conditions. Besides, several different combinations of closure models (i.e., closure models of fluid-particle drag, particle-particle interaction term, granular temperature, radial distribution function, etc.) have been used for carrying out the simulations. Many different combinations of MFM closure models (fluid-particle drag, radial distribution, frictional viscosity, etc.) have been verified and validated under varied conditions^{6,8,33}, as shown in Table 1. However, there is no specific recommendation for using a particular closure model for a given flow regime to accurately predict the segregation and intermixing effects.

This study analyzes different closure model combinations recommended in the literature for simulating LSFb to quantify and understand their role in segregation and intermixing.

Table 1. Evaluation of different simulations methodologies and closures used by researchers for investigating hydrodynamics polydisperse mixtures in LSFb

Reference	Cornelissen et al. ³	Reddy et al. ⁶	Khan et al. ⁸	Rahaman et al. ²⁸
Granular viscosity	Syamlal et al. ³⁴	Gidaspow et al. ³⁵	Gidaspow et al. ³⁵	Gidaspow et al. ³⁵
Granular viscosity	Lun et al. ³⁶	Lun et al. ³⁶	Lun et al. ³⁶	Lun et al. ³⁶
Frictional viscosity	Schaffer ³⁷	None	None	Schaffer ³⁷
Radial distribution	Ding and Gidaspow ³⁸	Ding and Gidaspow ³⁸	Lun et al. ³⁶	Ding and Gidaspow ³⁸
Granular temperature	Syamlal et al. ³⁴	Algebraic	Algebraic	Ding and Gidaspow ³⁸
Fluid-particle drag	Gidaspow ²⁴	Pandit and Joshi ²⁵	Gidaspow ²⁴	Syamlal O'Brien ²⁹ , Gidaspow ²⁴ and Wen and Yu ¹⁶
Particle-particle interactions	None	None	Syamlal ³⁹	Syamlal ³⁹

1.2 Objectives of the present study

As discussed in the previous sub-section, several computational studies in the published literature on intermixing and segregation characteristics of polydisperse LSFb. Most of the computational studies in the literature have been strictly restricted to binary LSFb. Very few studies in the published literature consider hydrodynamic simulations of LSFb systems consisting of more than two solid components²⁸. The objective of the present study is to evaluate the capabilities and limitations of the MFM to predict the segregation and intermixing behavior of polydisperse LSFb consisting of 2-6 sizes and densities of particle mixtures. Issues concerning the closure terms (frictional viscosity, fluid-solid drag, and particle-particle interaction) in the MFM simulations of LSFb have been critically analyzed. Extensive sensitivity analyses have been carried out to evaluate the advantages and disadvantages of performing MFM simulations for polydisperse LSFb. Under homogenous and heterogenous conditions, simulations have been carried out under laminar, transition, and turbulent flow

regimes. Conclusive guidelines have been provided based on the sensitivity analyses, which will help practicing engineers and technologists to carry out MFM simulations of polydisperse LSFb more rationally with caution.

2 CFD MODELING

2.1 Geometry and meshing

MFM simulations are favorably used in industries to study bed hydrodynamics for large-scale LSFb owing to the computational and economic feasibility that they offer. The MFM model has certain limitations. It treats the continuous and dispersed phases in an interpenetrating continuum, accounting for particle-particle and particle-fluid interactions in an ad-hoc manner. The high-precision computational approaches which treat the dispersed phases as discrete entities (such as CFD-DEM and Particle Resolved-Direct Numerical Simulations (PR-DNS)) are too expensive and time-consuming. Hence, their applications are limited to small and moderate-scale LSFb consisting of a few thousand particles only¹¹.

Even though the advancement of high-performance computation has enabled us to carry out complete three-dimensional CFD simulations of fluidization systems, these have been limited to small Reynolds numbers for a limited number of particles for dilute particle systems. When the purpose of CFD simulations is to design, scale-up, or optimize industrial-scale fluidized beds, two-dimensional simulations remain the preferred choice. 2D simulations provide satisfactory predictions of axial velocity profiles and void fractions. Thus, although fairly detailed three-dimensional CFD approaches exist for simulating fluidized beds, 2D simulations continue to be the most feasible option for quick estimates of large-scale LSFb hydrodynamics for industrial applications.

The section describing the geometry, mesh details, and boundary conditions used to define polydisperse LSFb is explained in detail in the supplementary material file. The details of the dimensions used for these three cases have been specified in Table 2. Three methodologies

were evaluated to identify their advantages and limitations reported in section 5 of the supporting information file. The results reported in this manuscript (other than those explicitly specified in section 2 of the supporting information file), have been carried out using the 3D cylindrical model, i.e., Geometry-3 shown in Table 2.

For all the geometries specified in Table 2, the inlet was prescribed as a uniform liquid superficial velocity, while the outlet was set to have a constant pressure (101,325Pa). The side-wall boundary conditions varied for the different cases, which have been shown in Table 2. As the MFM is being used, all the particle and fluid phases are in an interpenetrating continuum. Separate governing equations for the continuity and momentum were solved for each particle phase having different sizes/densities (details of these equations and the closure terms have been given the section 3 of the supporting information file). For example, four sets of governing equations were solved in any given ternary mixture case, three sets of equations for each of the three-particle phases, while one set for the liquid phase. The solid phases were patched with the overall solid volume fraction of 0.6 (i.e., for any given case, the sum of the initial packing fraction of all the solid species involved was equal to 0.6). All the simulations have been carried out with equally distributed volume fractions, i.e., for a ternary particle mixture, the volume fraction for each of the three solid species was 0.2. The initial packing height varied for each case and was determined from the corresponding literature data. The details of the governing equations and the closure models have been specified in the supplementary material file.

Table 2. Sensitivity analysis for bed description of polydisperse LSFb

Parameters	Geometry-1	Geometry -2	Geometry -3	Geometry -4
3D/2D	2D	2D	3D	2D
Diameter of the column	25mm	50mm	50mm	100mm
Column Height	1200 mm	1200 mm	1200 mm	800 mm
Side-wall boundary condition	Axisymmetric	No-slip	No-slip	No-slip

In all the simulated cases, the column to particle diameter ratio was greater than ~ 12 to eliminate the wall effects^{12,40}. A thorough grid independence test was done which showed that a 3D cylindrical model with uniform grids of 1mm size were suitable for the simulations. Grid independence study has been described in detail in section 1 of the supplementary material file.

2.2 Model specifications

The constitutive equations for frictional viscosity, fluid-particle drag, particle-particle interactions were used to model the interfacial interactions. Previous studies have indicated that the role of non-drag forces such as lift, added mass is negligible compared to the fluid-particle drag force (Cheng and Zhu¹; Cornelissen et al.³). Thus, in the present study, only fluid-particle drag force closure has been considered. The effect of other interfacial forces (i.e., non-drag interfacial forces) has been ignored. Four different drag fluid-solid models have been evaluated in the present study. However, unless explicitly specified, all the simulation results reported in the present study have been carried out using the Gidaspow²⁴ drag model as per the suggestion of Khan et al.⁸. All the other closure terms have been chosen as per the recommendations of Khan et al.⁸ (as listed out previously in Table 1) unless specified.

For the turbulent regime, the $k-\varepsilon$ model along with granular kinetic theory has been used. The standard $k-\varepsilon$ model for single-phase flows has been extended for the multi-component systems with additional terms that include interphase turbulent momentum transfer to consider the effects of turbulence. The standard $k-\varepsilon$ model has five empirical constants C_μ , $C_{\varepsilon 1}$, $C_{\varepsilon 2}$, σ_k and σ_ε in its formulation and their values are 0.09, 1.44, 1.92, 1.0 and 1.3, respectively. These standard values resolve the flow field in fluidized beds^{6,41,42} and have been used in the present work.

All terms of the governing equations for the unsteady state were discretized using the second-order upwind differencing scheme. The Courant number defines the step size in unsteady simulations. The step size is chosen to keep the Courant number always less than 0.006. The

SIMPLE algorithm was employed for the pressure-velocity coupling. The convergence criterion (sum of normalized residuals) is set at 1×10^{-4} for all the equations. The CFD simulations predict the local values of phase hold-ups and their distributions in the bed, liquid phase flow patterns, intermixing levels of the individual phases, and turbulence characteristics. The reported volume fraction data in each simulation is time-averaged volume fraction obtained after the simulation reaches a steady state. The steady-state is defined as the stage after which the change in volume fraction profile is less than 2 percent if the simulation is continued. The time required for a simulation to reach a steady-state varies from system to system (some systems were found to exhibit steady-state at as low as ~ 100 s while others reach steady-state at ~ 200 s). The simulations were continued for 50 s to time-average the data once the steady-state was reached. The exported volume fraction data for particular species at each node is then space averaged over the axial location to obtain a single value of volume fraction of the species at given axial locations.

3 RESULTS AND DISCUSSION

The segregation and intermixing in LSFB have been studied extensively for binary particle mixtures. Some investigations in the published literature also focus on higher polydispersity particle mixtures along with binary particle mixtures. Section 4 in the supplementary material file lists out various binary and higher polydispersity LSFB systems, respectively. For rigorous and robust testing of the various MFM closure models. Simulations have been carried out with practically all the binary and higher polydispersity LSFB segregation and intermixing studies reported in the published literature.

3.1 Validation studies

The continuous phase axial volume fraction was evaluated for different binary and higher polydispersity cases under consideration. Figure 1 shows the axial variation of solid volume fraction for a binary particle mixture at four different superficial liquid velocities. The binary

particle mixture has the same particle size distribution ($d_{mean} = 1.09$ mm), while the particle densities of the two solid species are 1900 and 1600kg/m³, respectively. The predicted axial variation of solid volume fractions for 1900 and 1600kg/m³ solids is in reasonable agreement with the experimental data. From Figure 1 (A), it can be observed that the experimental data does show a small intermixing zone between the two-particle phases. In contrast, the CFD predicted solid fractions show a sharp interface between the light and heavy particle phases, indicating no intermixing. The distance along which the mixing zone is present in LSFB increases with an increase in the superficial liquid velocity (see experimental data of Figure 1 (b), (c), and (d)). However, the CFD predictions still show a clear interface between the particle phases and do not predict the mixing zone.

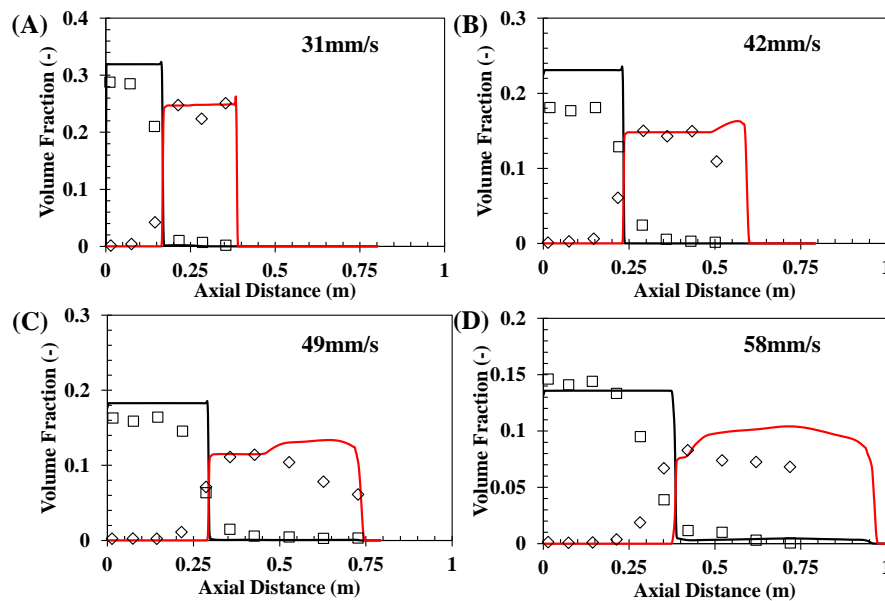


Figure 1. Comparison of the axial solid hold-up profiles predicted from CFD against experimental results of Galvin et al.¹⁸ for a binary particle mixture.

Besides the above studies, validations were also done for other parameters in polydisperse LSFB which have been described in section 5 of the supplementary material. From the above-conducted validation studies, it is clear that the MFM can predict the hydrodynamics of a polydisperse LSFB to a great extent. The extensive simulations carried out in the present study

over a wide range of flow regimes helped to acknowledge the limitations of the MFM for simulating the polydisperse, which have been pointed out and quantified in the later sections.

3.2 Bed expansion characteristics

The experimental study of Juma and Richardson⁴³ carried out for a binary particle mixture LSFBS has been chosen to evaluate the bed expansion characteristics. The simulations were carried out over four superficial liquid velocities to cover all the segregation and intermixing stages. Figure 2 represents the case for binary particle mixture. Both the particle species have the same particle density (2960 kg/m^3), while the sizes of the bigger and smaller particle species are 4mm and 3mm, respectively, i.e., a size ratio of 1.333. As evident from Figure 2 (A), the smaller-sized particles segregate and settle on top of the layer of larger size particles for the superficial liquid velocity of 73mm/s. As the superficial liquid velocity is increased to 109mm/s (Figure 2 (B)), partial intermixing occurs between the two-particle species.

Further increase of superficial liquid velocity leads to increased intermixing zone (Figure 2 (C) and (D)). Figure 6 (A) –(B) also has embedded contour plots along the YZ plane of the mean volume fraction for the four superficial liquid velocities to better visualize the segregation and intermixing. The results presented in Figure 2 show that the superficial liquid velocity at which the LSFBS is operated, i.e., the operating flow regime, plays a vital role in imparting segregation and intermixing behavior to the particle phases under consideration.

Figure 3 and Figure 4 show the axial variation of mean volume fraction for LSFBS consisting of 3mm - 2mm (i.e., size ratio = 1.5) and 4mm - 2mm (i.e., size ratio = 2) solid particle species. The simulations were carried out for the same four superficial liquid velocities as the 4mm and 3mm binary LSFBS. A comparison of Figure 3 and Figure 4 with Figure 2 reveals that intermixing occurs at a comparatively lower superficial liquid velocity for the low particle size ratios (i.e., the size ratio of 1.333 in the present case). Besides, the intermixing zone for the low particle size ratios is significantly larger than that exhibited by the high particle size ratios. The

experimental results of Chavan and Joshi²⁰ state that for constant density binary particle mixtures (i) if the size ratios are less than 1.4, complete intermixing takes place, (ii) if the size ratios are in between 1.4 and 1.55, partial intermixing takes place and (iii) if the size ratios are greater than 1.55, complete segregation would occur. While the results obtained from the present MFM simulations corroborate the size ratio ranges put forward by Chavan and Joshi²⁰, they further signify that, along with the size ratios, the segregation and intermixing phenomena also depend on the superficial liquid velocity at which the LSFBS is operated. Thus, polydisperse LSFBS with size ratios greater than 1.55 can also show intermixing behavior when operated at higher superficial liquid velocities, as shown in Figure 4(C) and (D).

Since the binary particle mixture LSFBS simulations were reported for the combinations of 4mm-3mm, 3mm-2mm, and 4mm-2mm, it was thought desirable to combine these three particle sizes and investigate the bed expansion characteristics. The axial variation of solid volume fraction for the ternary mixture of 4mm-3mm-2mm has been reported in Figure 5.

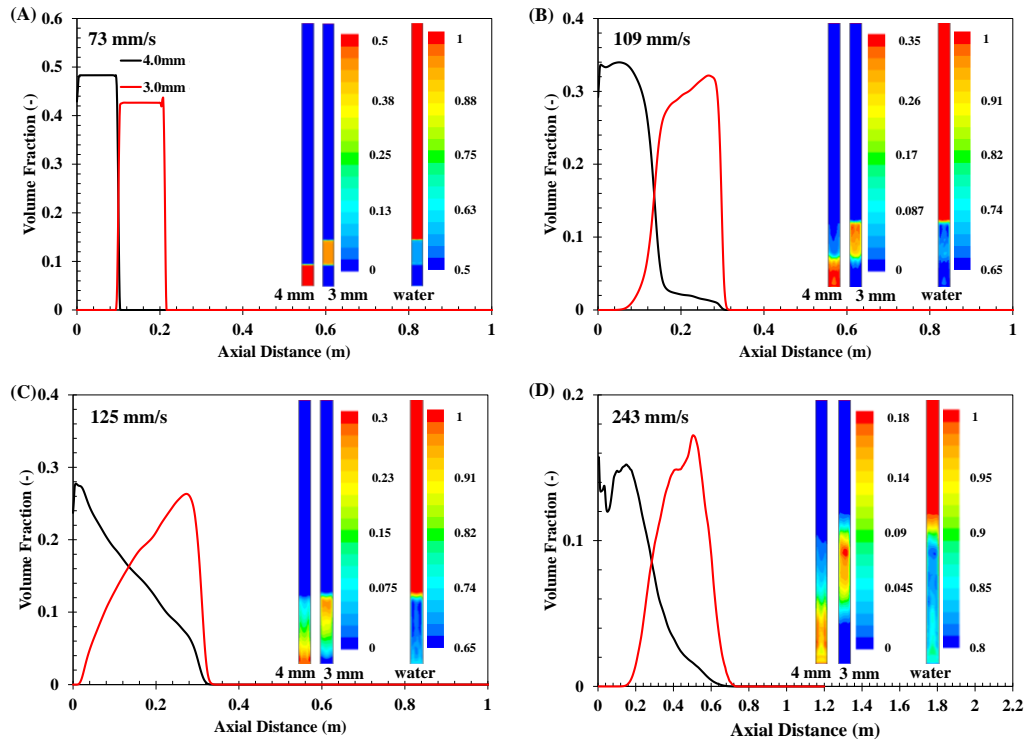


Figure 2. Solid volume fraction predicted from MFM for binary particle mixture of sizes 4mm and 3mm (A) $V_L = 73$ mm/s (B) $V_L = 109$ mm/s (C) $V_L = 125$ mm/s (D) $V_L = 243$ mm/s

For the low superficial liquid velocity ($V_L = 73\text{mm/s}$), the three particle mixtures arrange themselves as three distinct layers (with little to no intermixing) at the top of each other, starting from the largest size (4mm) at the bottom-most layer followed by the mid-size particles (3mm). The smallest size particles (2mm) settled at the topmost layer, as observed from Figure 5(A). Thus, the mean solid volume fractions at 73mm/s for the ternary mixture showed the segregation phenomena with the overall bed expansion height similar to that of binary particle mixtures (4mm-3mm, 3mm-2mm, and 4mm-2mm) as illustrated previously in Figure 2(A), Figure 3(A) and Figure 4(A).

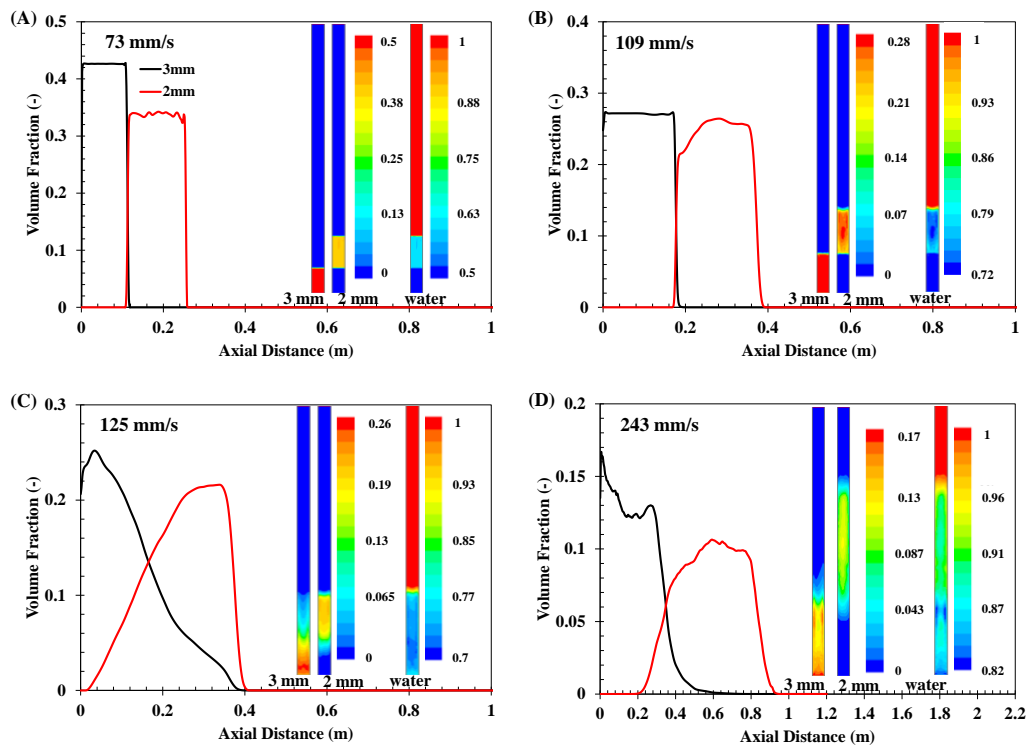


Figure 3. Solid volume fraction predicted from MFM for binary particle mixture of sizes 3mm and 2mm (A) $V_L = 73\text{ mm/s}$ (B) $V_L = 109\text{ mm/s}$ (C) $V_L = 125\text{ mm/s}$ (D) $V_L = 243\text{mm/s}$

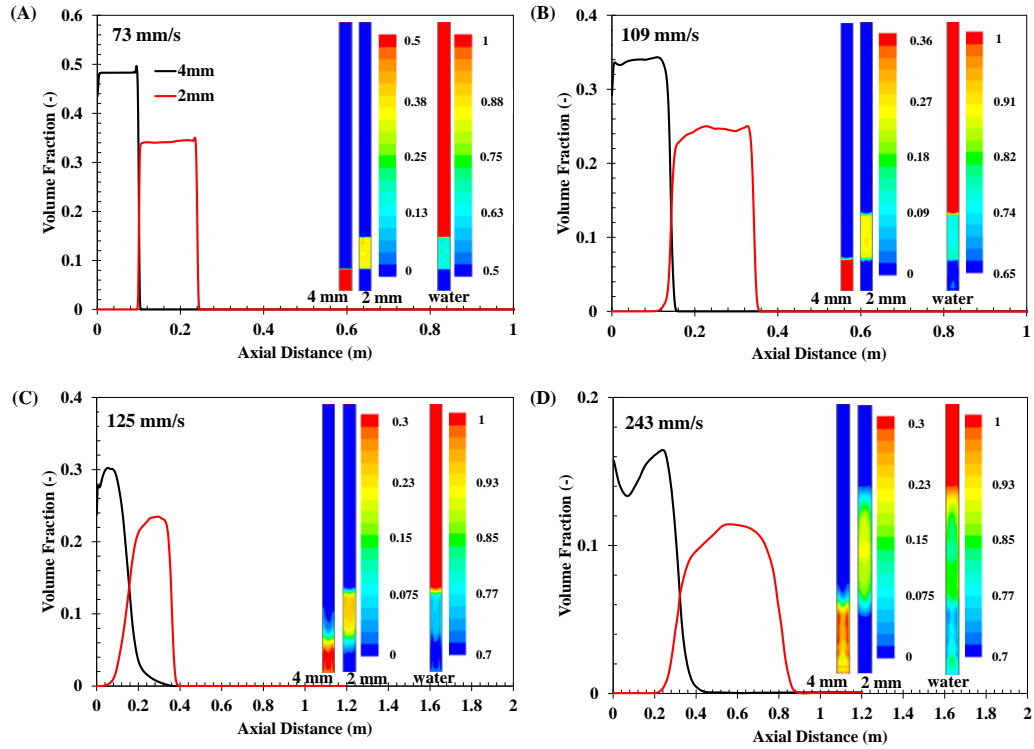


Figure 4. Solid volume fraction predicted from MFM for binary particle mixture of sizes 4mm and 2mm (A) $V_L = 73$ mm/s (B) $V_L = 109$ mm/s (C) $V_L = 125$ mm/s (D) $V_L = 243$ mm/s

The mean solid volume fraction plots for the bed operating at 109mm/s are illustrated in Figure 5 (B). The axial volume fraction plot in Figure 5 (B) shows that the 4mm and 2mm particles completely segregate, whereas the 4mm and 3mm particle sizes intermix to some extent. Similar segregation and intermixing characteristics were also exhibited by the 4mm-3mm and 4mm-2mm binary particle mixtures, as shown in Figure 2(B) and Figure 4(B), respectively. The binary particle mixture of 3mm-2mm had shown little to no intermixing at 109 mm/s. However, the intermixing zone of the 3mm and 2mm particles in the ternary mixture of 4mm-3mm-2mm at the same superficial liquid velocity (109mm/s) is seen to increase significantly. The difference in the intermixing zone predicted for the binary, and ternary particle mixtures infer that adding another (bigger or smaller size) particle species may significantly change the solid volume fractions, thereby leading to substantial changes in the segregation and intermixing characteristics.

Further, an increase in the superficial liquid velocity to 125mm/s and then to 243mm/s in the ternary particle mixture (shown in Figure 5 (C) and (D), respectively) show segregation and intermixing behavior similar to that offered by their binary counterparts.

Simulations were also carried out for a quaternary particle mixture by introducing a new particle species of size 2.2mm, i.e., the size ratio of 1.818 with 4mm particles, 1.3636 with 3mm particles, and 1.1 with 2mm particles. As shown in Figure 6 (A), for 53mm/s, the 4mm-3mm, 4mm-2mm, and 3mm-2mm particle species combinations continued to show segregation as they did for the ternary particle mixture cases. The 2.2mm particle mixture showed complete segregation with the 4mm and 3mm particles (i.e., size ratios 1.818 and 1.3636).

In comparison, they did show a small intermixing zone with the 2mm particles (i.e., size ratio 1.1). Complete intermixing was observed for the 2.2mm-2mm particles for increased superficial liquid velocity, i.e., at 109mm/s, as shown in Figure 6 (B).

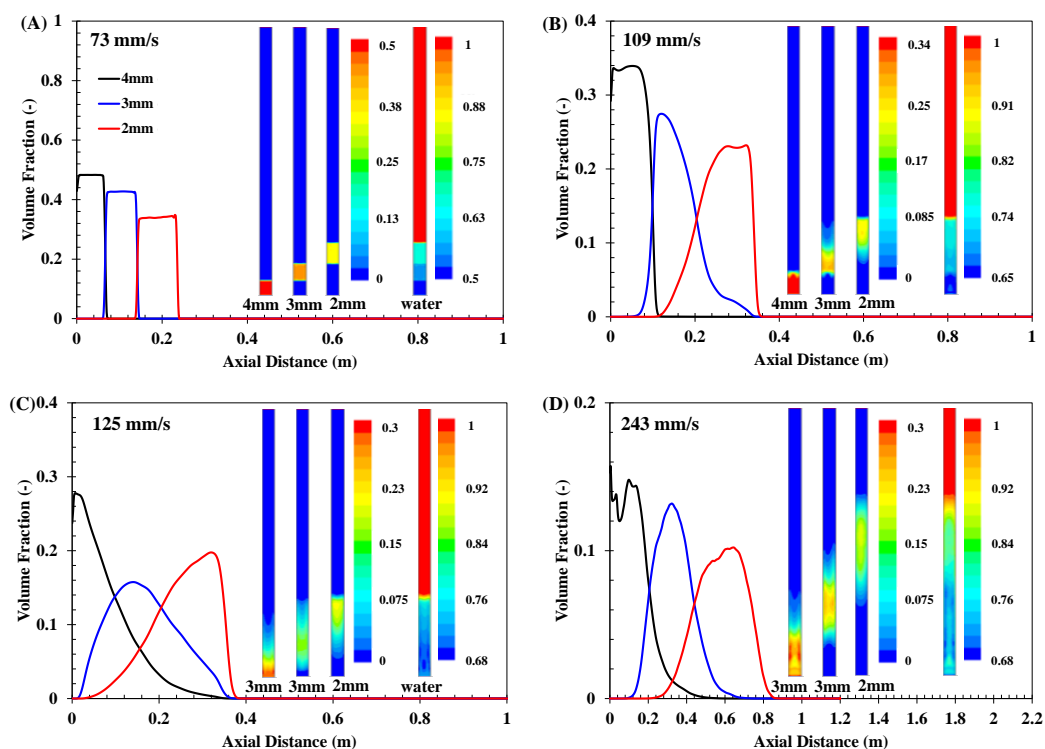


Figure 5. Solid volume fraction predicted from MFM for ternary particle mixture of sizes 4mm, 3mm and 2mm (A) $V_L = 73$ mm/s (B) $V_L = 109$ mm/s (C) $V_L = 125$ mm/s (D) $V_L = 243$ mm/s

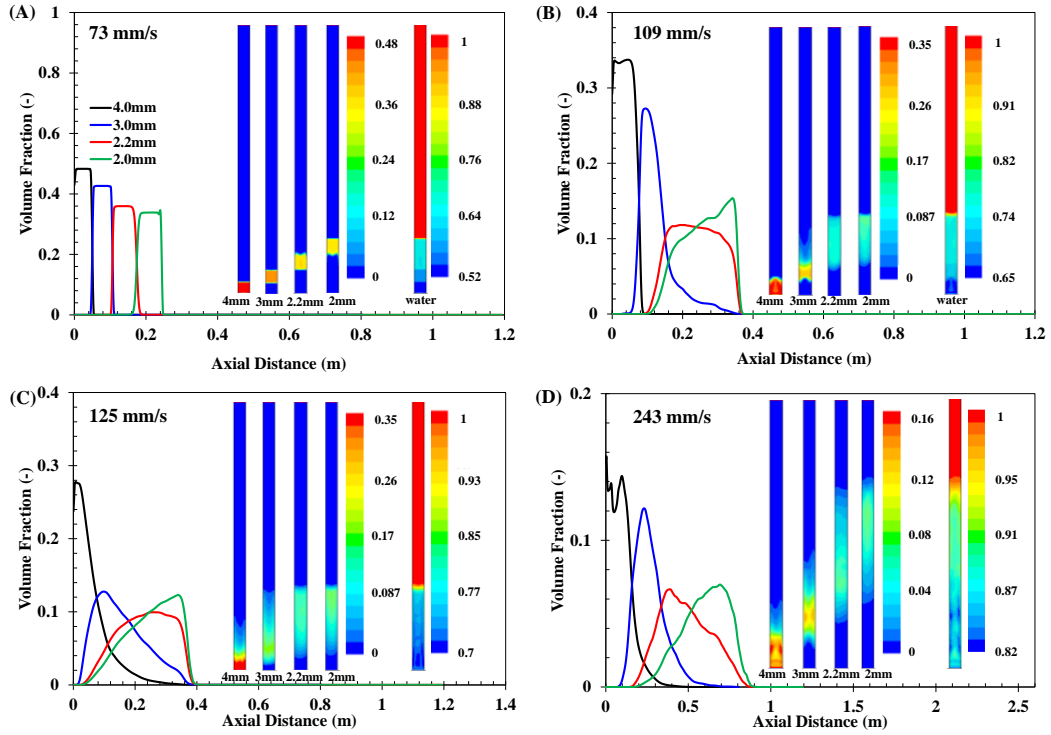


Figure 6. Solid volume fraction predicted from MFM for quaternary particle mixture of sizes 4mm, 3mm, 2.2mm and 2mm (A) $V_L = 73$ mm/s (B) $V_L = 109$ mm/s (C) $V_L = 125$ mm/s (D) $V_L = 243$ mm/s/simulations of the MFM

Also, for 109mm/s, 3mm particles showed partial intermixing with 2.2mm and 2mm particle species. The 4mm particles continued to show partial intermixing with the 3mm particles at 109mm/s, while they exhibited complete segregation with the 2mm and 2.2mm particle species. Increased intermixing zones were observed for all the particle species with a further increase in superficial liquid velocities, as shown in Figure 6 (C) and (D).

3.3 Evaluation of the closure models

In this section, simulations were carried out using different closure models as previously listed in Table 1 and suggested in other published literature³⁰. MFM model was used to evaluate the accurateness of simulations by comparing them against experimental data of Galvin et al.¹⁸ using the Gidaspow²⁴ fluid-particle drag model. Firstly, the simulations were carried out to evaluate the effect of frictional viscosity closure models and the particle-particle interaction closure models. Figure 7 and Figure 8 illustrate the volume fraction contour plots for the heavier particle phase (1900kg/m^3) and the lighter particle phase (1600kg/m^3). The heavy to

light particle density ratio is 1.1875 and has already been shown in Figure 1 (a) (and shown experimentally by Galvin et al.¹⁸). The particles completely segregate when the LSFB is operated at a superficial liquid velocity of 31mm/s. Figure 7 and Figure 8 all show that the MFM simulations can predict the segregation characteristic reasonably accurately. The steady-state solid hold-ups and the heights of the two-particle phases predicted using the three closure model combinations are similar. However, the complete segregation behavior sets in quicker (at ~60 secs) for the third combination (i.e., wherein neither the frictional viscosity nor the particle-particle interactions were considered) as compared to the other two closure model combinations (at ~80 secs).

Thus, whether or not closure models account for the frictional viscosity and the particle-particle interactions, the MFM can predict the segregation of particles for the LSFB. Similarly, simulations carried out for cases where intermixing of particles occur also confirm that the mean solid volume fractions of the solid and liquid phases are identical, whether or not the Schaffer³⁷ frictional viscosity model and the Syamlal³⁹ particle-particle interaction closure models are used. The only difference between simulations where particle-particle interaction closure models are not considered is that the time required for the LSFB to attain a steady-state is comparatively less (as it did even for the LSFB, which showed complete segregation (Figure 7 and Figure 8)).

The granular temperature of the solid phases, which is a measure of the kinetic energy due to the random oscillations of the solids, is an excellent parameter to evaluate the accurateness of particle-particle interactions. The granular temperature values are very low, as evident from Figure 9 (A-C) for the experimental data of Galvin et al.¹⁸, which exhibited complete segregation of the two-particle species. The granular temperatures of 4mm and 3mm binary particle mixture, operating at a superficial liquid velocity of 243 mm/s, is plotted in Figure 9.

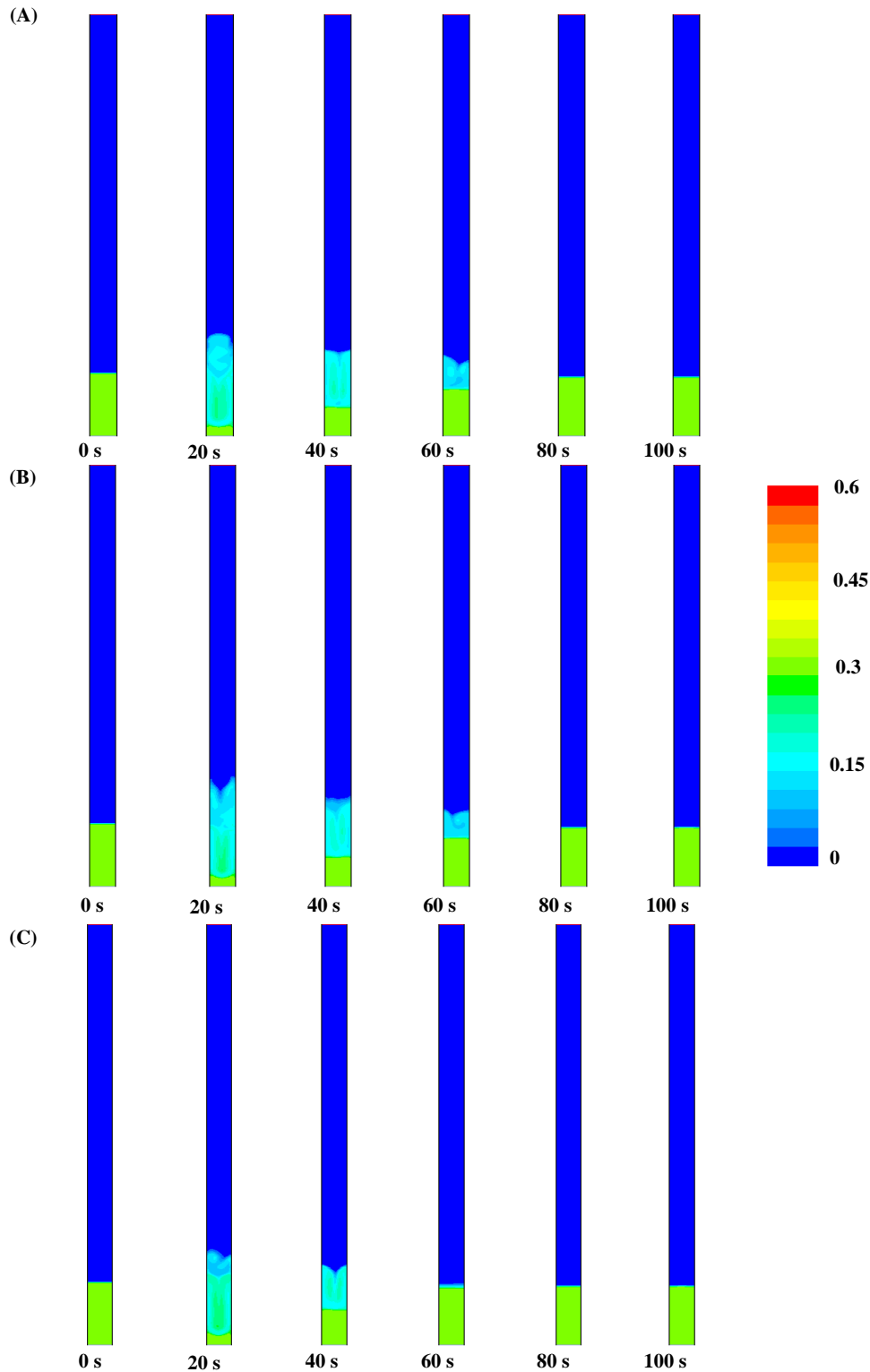


Figure 7. Solid volume fraction contour plots for particles of density 1900kg/m^3 in a binary LSF of (Case 1: $\rho_{s_1} = 1900\text{kg/m}^3$ and $\rho_{s_2} = 1600\text{kg/m}^3$, $d_{s_1} = d_{s_2} = 1.01\text{mm}$) at $V_L = 31\text{mm/s}$ using Gidaspow drag model with (A) Syamlal³⁹ particle interaction model but no frictional stresses model (B) Syamlal³⁹ particle interaction model and Schaeffer³⁷ frictional viscosity model (C) No particle interaction model or frictional stress model.

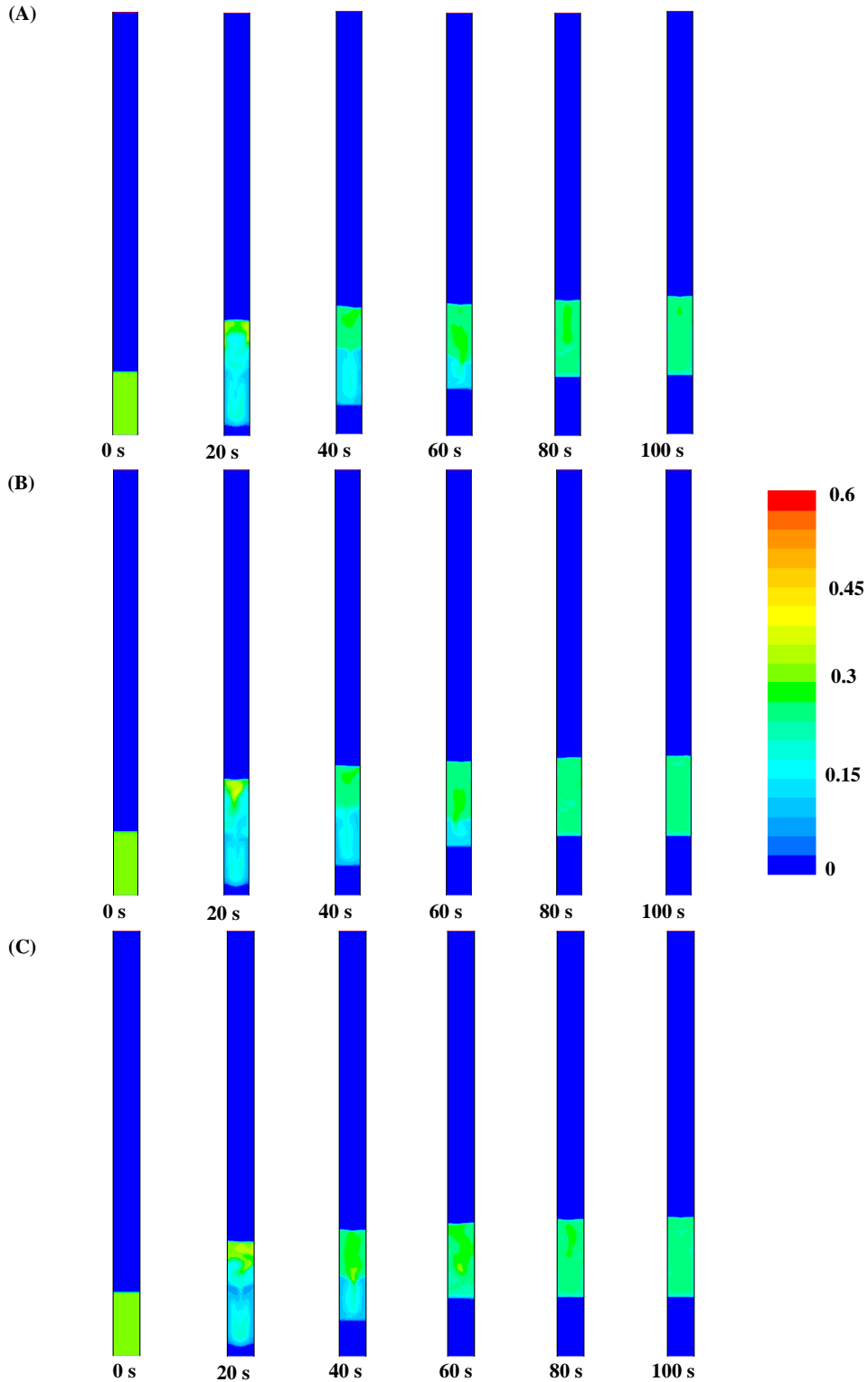
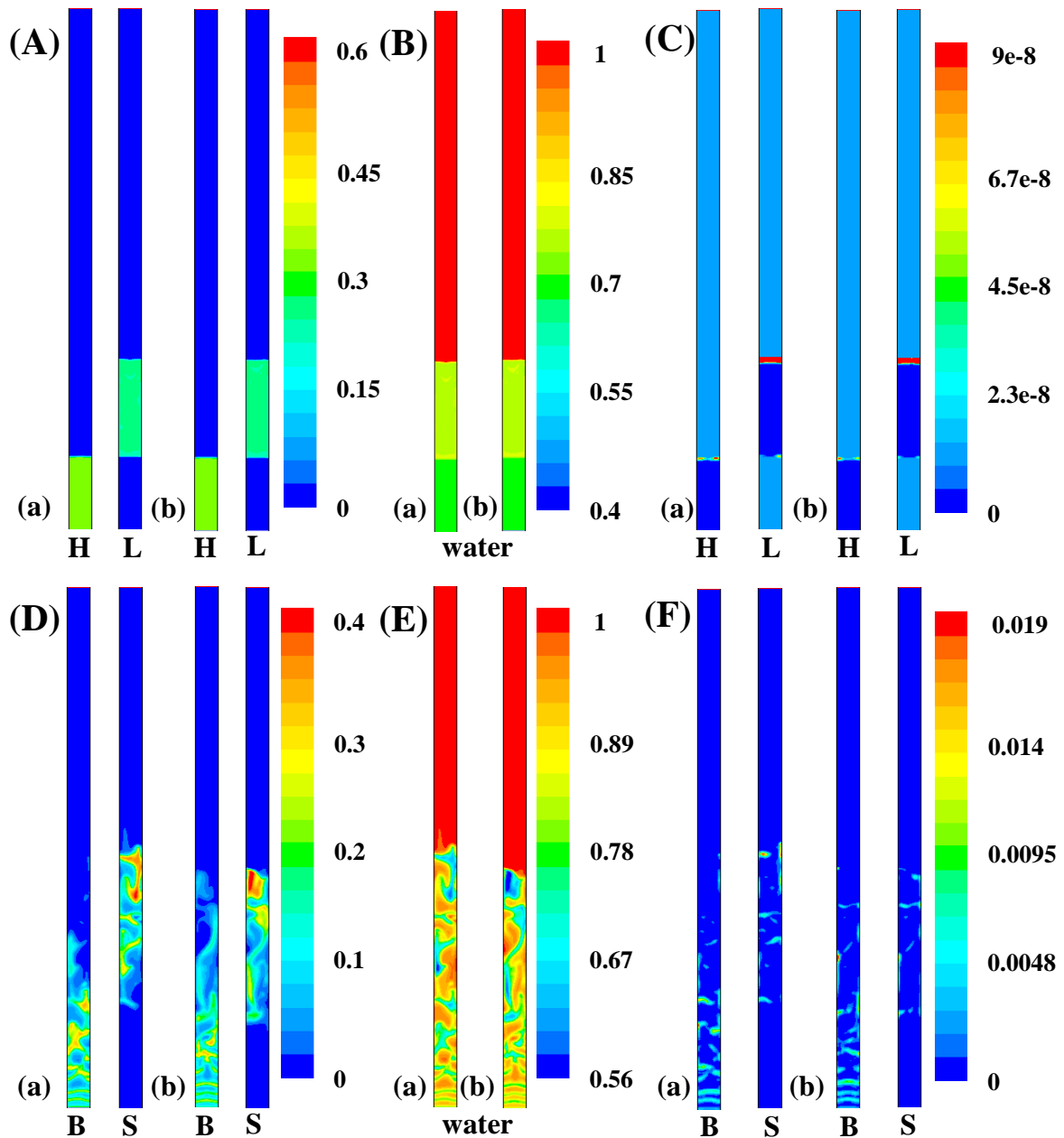


Figure 8. Solid volume fraction contour plots for particles of density 1600kg/m^3 in a binary LSF (Case 1: $\rho_{s_1} = 1900\text{kg/m}^3$ and $\rho_{s_2} = 1600\text{kg/m}^3$, $d_{s_1} = d_{s_2} = 1.01\text{mm}$) at $V_L = 31\text{mm/s}$ using Gidaspow drag model with (A) Syamlal³⁹ particle interaction model but no frictional stresses model (B) Syamlal³⁹ particle interaction model and Schaffer frictional stresses model (C) No particle interaction model or frictional stress model.



(a) without particle-particle interaction closure term
 (b) with Syamlal O'Brien symmetric particle-particle interaction closure
 H: heavy particle L: light particle B: big particle S: small particle

Figure 9. (A) Contours of instantaneous solids fraction [dimensionless], (B) contours of instantaneous liquid fraction [dimensionless], (C) contours of granular temperature [units are in m^2/s^2], and, for a LSFB with $1900\text{kg}/\text{m}^3$ and $1600\text{kg}/\text{m}^3$ particle density binary mixture operating at $31\text{mm}/\text{s}$ extracted after 100 seconds of simulation (i.e. after steady state has been achieved). (D) Contours of instantaneous solids fraction [dimensionless], (E) contours of an instantaneous liquid fraction [dimensionless], (F) contours of granular temperature [units are in m^2/s^2], and, for an LSFB with 4mm and 3mm particle sizes binary mixture operating at $243\text{mm}/\text{s}$ extracted after 100 seconds of simulation (i.e., after steady state has been achieved)

Figure 9 (F) shows that granular temperature does not significantly affect whether or not the particle-particle interaction closure models are used. For the case illustrated in Figure 9 (D-F), the particle Reynolds number based on the terminal settling velocity ($Re_{Si} = d_{Si} V_{Si\infty} \rho_L / \mu_L$) for the larger particle size is $Re_{S1} = 2080$ and for the smaller particle size is $Re_{S2} = 1260$. This means that the LSFB under consideration is under turbulent conditions. Besides, as shown in Figure 9 (E), the liquid volume fraction is high enough for the system to be in the heterogeneous flow regime. As reported earlier by Peng et al.²⁷, when the flow regime is turbulent and the LSFB exhibits a heterogeneous nature, the fluid-particle drag determines the solid dispersion while the particle-particle interactions play little to no role. Thus, for this particular case (shown in Figure 9(D-F)), the correct prediction of the fluid-particle drag alone confirms the prediction accuracy of solid dispersion and thereby the segregation and intermixing.

The sensitivity of particle-particle closures analyzed from Figure 7, Figure 8, and Figure 9 infers that the existing particle-particle closure model (i.e., Syamlal³⁹ model) used to account for the particle-particle interactions may possess certain physical limitations in accurately predicting the solid dispersion.

An interesting point that needs to be noted here is that the Syamlal³⁹ model is predominantly used to model gas-solid granular systems⁴⁴. The gas-solid systems exhibit a much higher degree of heterogeneity due to the aggregating bubbling and slugging phenomena. On the other hand, the LSFB does not show such intense bubbling and slugging phenomena. Thus, the hydrodynamic behavior of gas-solid systems is quite different from liquid-solid systems. The exact differences in the role of particle-particle interactions for gas-solid and liquid-solid flows need to be evaluated by investigating these systems using high-fidelity numerical and experimental techniques. The closure terms for MFM that would result based on rationally quantified particle interactions would help achieve more accurate predictions of the solid hold-up profiles of polydisperse particle LSFB.

3.4 Limitations of the MFM simulations

The limitations of the particle-particle interaction predictions for LSFBS brought forward in this study need to be evaluated to identify the limitations of the proposed MFM simulation strategies. For this purpose, four specific LSFBS systems were chosen from the literature. The experiments conducted on these systems have already shown that they exhibit partial or complete intermixing characteristics¹⁸⁻²⁰. The results (from the MFM simulations) of axial variation of solid fraction for these four LSFBS systems have been plotted in Figure 10. The comparison of the MFM predicted solid fractions against the experimental data (shown in Figure 10) indicates that the MFM simulations could not predict the intermixing zones for all four cases. The inability of MFM to accurately predict the intermixing of particles point out two possibilities: (i) limitations of the Syamlal O'Brien symmetric model (which has been already identified earlier in this study), and (ii) limitations of the fluid-particle drag closures leading to inaccurate distribution of solids. To evaluate the role of fluid-particle drag closures, simulations for the senary particle mixture LSFBS of Murli et al.¹⁹ were carried out using three different drag models (other than the Gidaspow). These drag models were chosen because they have been previously reported to yield accurate segregation and intermixing predictions for LSFBS consisting of different binary particle mixtures^{6,28,30}. The simulations conducted using the Syamlal O'Brien²⁹ model yielded complete segregation behavior exactly similar to that shown in Figure 10 (D) using the Gidaspow drag model (and thus have not been reshowed). Figure 11 (A) and (B) illustrate that even when the Rong et al.³² and the Pandit and Joshi²⁵ drag models are used, the predicted axial variation of solid volume fractions still shows complete segregation with little to no intermixing behavior.

The largest particle species settled at the bottom-most bed layer while the subsequent particle sizes settled over each other sequentially. Thus, even when physically more accurate drag models were used, the six particle phases were segregated as they did in Figure 10 (D) with

slight variations in the height of bed expansion of each particle phase. If we look at the experimentally reported particle Reynolds number of the six particle species investigated in the study of Murli et al.¹⁹, they are: (i) $Re_{S1} \approx 22.85$, (ii) $Re_{S2} \approx 17$, (iii) $Re_{S3} \approx 12$, (iv) $Re_{S4} \approx 8$, (v) $Re_{S5} \approx 6$, and (vi) $Re_{S6} \approx 3.5$. This means that all selected Re_{Si} lie in the laminar regime where particle-particle interaction governs the LSFB hydrodynamics²⁷. Thus, changing the fluid-particle drag still does not result in any intermixing, as shown in Figure 11 (A) and (B). It has already been shown in the previous section that the Syamlal³⁹ particle interaction model does not accurately account for the particle-particle interactions.

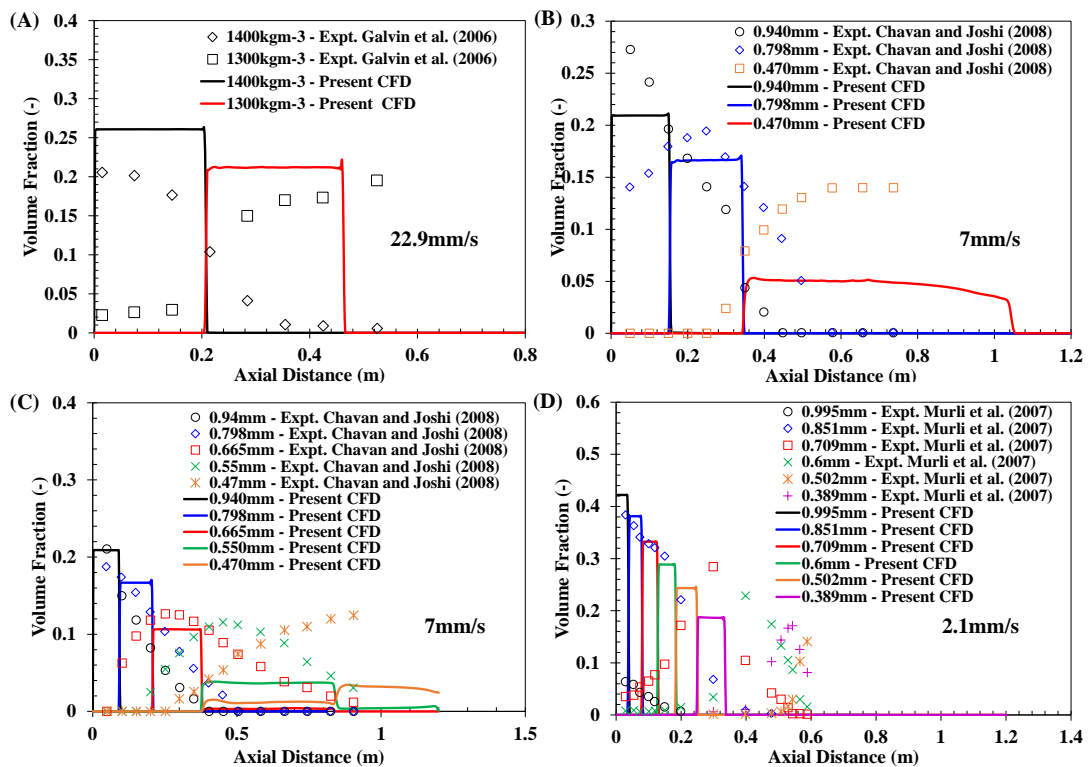


Figure 10. Comparison of solid volume fraction predicted from MFM against the experiments. (A) A binary mixture of Galvin et al.¹⁸ (B) Ternary mixture of Chavan and Joshi²⁰ (C) Quinary mixture of Chavan and Joshi²⁰ (D) Senary mixture of Murli et al.¹⁹

Thus, from the current study, the used closure models for particle-particle interactions are insufficient for accurate quantifications, which causes the particle mixtures to show dominant segregation behavior with little to no intermixing. The particle-particle interactions are one of the chief reasons for limitations in predicting the accurate axial distribution of polydisperse

particles. Evaluation of other closure terms such as pseudo-turbulence, frictional stresses, granular energy dissipation is missing in the liquid-solid multiphase flow literature. In particular, importance should be given to pseudo turbulence as it plays an important role in predicting accurate, granular temperatures otherwise under-predicted by MFM. Our group has previously shown that granular energy significantly affects bed hydrodynamics, even under laminar and homogenous flow regimes⁴⁵. The inclusion of an appropriate pseudo-turbulence closure term accurately accounts for the granular energy in MFM simulations⁴⁵. The increased computational power has made it possible to perform DNS simulations for obtaining physically appropriate closure terms for pseudo-turbulence, frictional stresses, particle-particle interactions, and granular energy dissipation. The limitations of the existing MFM in predicting intermixing behavior for polydisperse particle mixtures can be overcome by developing precise closure terms for various flow regimes from DNS.

In this direction, we have already started taking the results from the present study ahead and combining them with our in-house Immersed Boundary Method (IBM) solver⁴⁶, CFD-DEM solver⁹, and anisotropic Gaussian E-E solver⁴⁷.

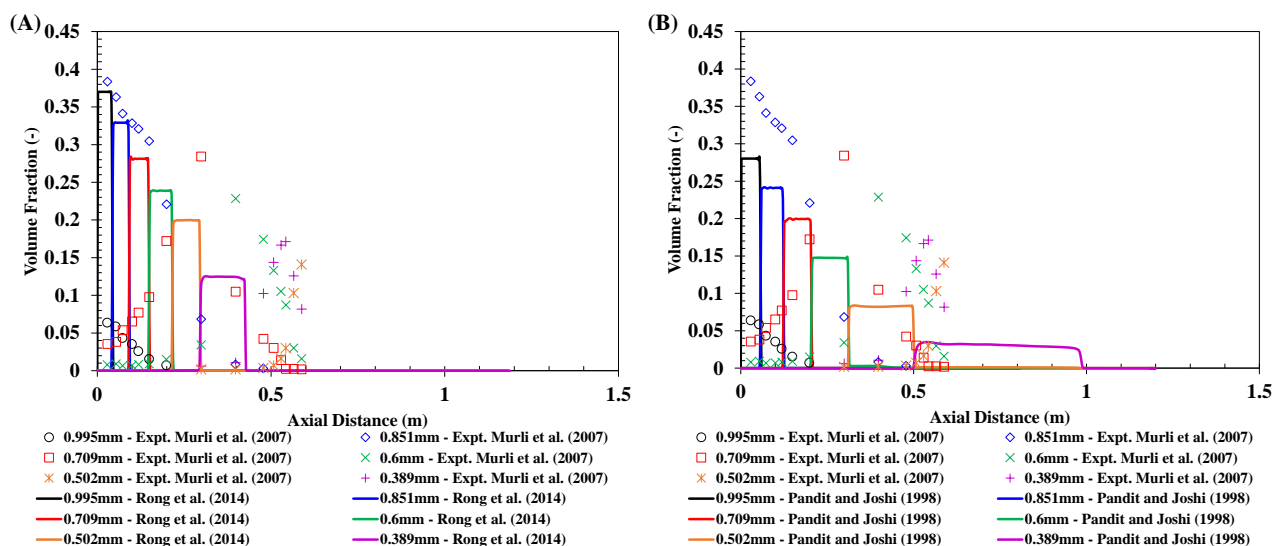


Figure 11. MFM simulation for the LSFBC consisting of binary particle mixture (reported experimentally by Murli et al.¹⁹) using (A) Rong et al. drag model³² (B) Pandit and Joshi²⁵ drag model.

3.5 Flow regime mapping using MFM

As shown in the previous sections, the limitation of the particle-particle interaction closures is evident. The flow regime has set a criterion to identify the polydisperse LSF configurations that can and cannot be correctly simulated using the proposed MFM model. The regime map illustrated in Figure 12 is generated based on the available experimental data from literature combined with the extensive simulations carried out in the present study.

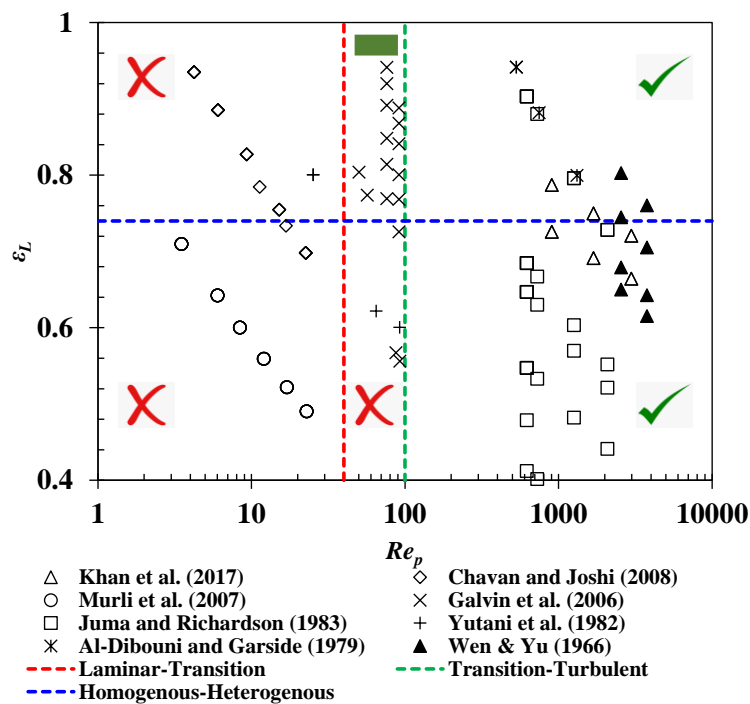


Figure 12. Regime map signifying the success and failure of the segregation and intermixing prediction of polydisperse particle mixtures using the MFM simulations.

In Figure 12, the liquid phase volume fractions predicted using the Richardson-Zaki¹³ equation have been plotted against the experimentally reported particle Reynolds's number (Re_s) for various polydisperse LSF configurations from published literature. The demarcation lines for the laminar-transition regimes (red line), transition-turbulent regimes (green line), and homogeneous-heterogeneous flow (blue horizontal line) have been illustrated in Figure 12. The red-cross and the green-tick markings shown in Figure 12 demonstrate the success and failure of the MFM to quantitatively predict the segregation and intermixing phenomena of LSF operating under that particular regime. The green-hyphen shown in the transition regime for

the heterogeneous regime signifies that the bed expansion characteristics can only be qualitatively predicted in this regime. Thus, the simulations carried out in the present study aided in deciphering the role of particle-particle interactions. The limitations that the existing particle-particle closure models possess for accurately predicting segregation and intermixing in LSFB consisting of polydisperse particle mixtures have been brought forward.

4 CONCLUSIONS

In this paper, the use of the multifluid model (MFM) in predicting the segregation and intermixing in LSFB consisting of binary and higher polydispersity particle mixtures varying in particle size and density has been demonstrated. A particular focus of this work was to decipher the role of the fluid-particle drag, frictional viscosity, and the particle-particle interaction closure models. The results from the MFM simulations conducted to evaluate the role of various closure models led to the following conclusions

(I) The frictional viscosity does not play a significant role in imparting bed expansion of LSFB and thus can be ignored.

(II) The particle-particle interactions play a vital role in the dispersion of solid particles for a laminar flow regime under homogenous flow conditions. The existing closure models for particle-particle interactions cannot accurately predict the segregation and intermixing phenomena under laminar and even transition regimes under homogenous flow conditions. The main reason for the limitation of the particle-particle interaction model is that they have been predominantly designed for dense gas-solid multiphase flows, which generally exhibit a much higher degree of heterogeneity. Liquid-solid multiphase flows (particularly in the laminar and homogenous regimes) show very different characteristics than the gas-solid systems. The exact differences in the role of particle-particle interactions for gas-solid and liquid-solid flows need to be evaluated by investigating these systems using high-fidelity numerical and experimental techniques. The closure terms for MFM that would result from rationally quantified particle

interactions would help achieve more accurate predictions of the solid hold-up profiles of polydisperse particle LSFBS.

(III) The dispersion of the solids in the heterogeneous flow conditions under turbulent and transition regimes are governed by the fluid-particle drag. The particle-particle interaction closures are not that significant under such conditions. The four fluid-particle drag closures from the literature, (i) Gidaspow, (ii) Syamlal O'Brien, (iii) Pandit and Joshi²⁵, and (iv) Rong et al.³², were able to predict the segregation and intermixing accurately under turbulent and heterogeneous flow conditions. These models could reasonably predict the overall bed expansion heights (especially for binary particle mixtures). The axial dispersion of individual species showed overprediction of segregation with little to no intermixing. Thus, a need is discerned for obtaining rational closure terms (for particle-particle interactions, pseudo-turbulence, and frictional stresses) for LSFBS extracted from Direct Numerical Simulations (DNS) of liquid-solid multiphase flow. Such rationally developed closure models would allow better and accurate predictions of axial solid fractions in polydisperse LSFBS.

(IV) A flow regime map signifying the success and failure of the MFM simulations has also been proposed in the present study. This flow regime map will help practicing chemical engineers and technologists determine whether the proposed MFM methodology will yield accurate results for any polydisperse LSFBS.

In addition, the present study also showed that 2D axisymmetric, 2D full bed (with no-slip boundary conditions on the walls), and 3D simulations, all three, were able to predict the segregation and intermixing studies for the LSFBS under consideration. Furthermore, the bed expansion studies showed that segregation and intermixing characteristics exhibited by ternary, quaternary (and higher polydispersity particle mixtures) at a given superficial liquid might vary from that offered by their binary particle mixture combinations.

ACKNOWLEDGMENTS

Shashank S. Tiwari acknowledges the fellowship support and computational resources given by Guangdong Technion-Israel Institute of Technology to conduct this work.

CONFLICT OF INTEREST

The author(s) declare(s) that there is no conflict of interest regarding the publication of this article.

DATA AVAILABILITY STATEMENT

The datasets generated during and analyzed during the current study are available from the corresponding author on reasonable request.

REFERENCES

1. Cheng Y, Zhu J-X (Jesse). CFD Modelling and Simulation of Hydrodynamics in Liquid-Solid Circulating Fluidized Beds. *The Canadian Journal of Chemical Engineering*. 2005;83(2):177-185.
2. Lettieri P, Di Felice R, Pacciani R, Owoyemi O. CFD modelling of liquid fluidized beds in slugging mode. *Powder Technology*. 2006;167(2):94-103.
3. Cornelissen JT, Taghipour F, Escudié R, Ellis N, Grace JR. CFD modelling of a liquid–solid fluidized bed. *Chemical Engineering Science*. 2007;62(22):6334-6348.
4. Ghatage SV, Peng Z, Sathe MJ, et al. Stability analysis in solid–liquid fluidized beds: Experimental and computational. *Chemical Engineering Journal*. 2014;256:169-186.
5. Doroodchi E, Galvin KP, Fletcher DF. The influence of inclined plates on expansion behaviour of solid suspensions in a liquid fluidised bed — A computational fluid dynamics study. *Powder Technology*. 2005;160(1):20-26.
6. Reddy RK, Joshi JB. CFD modeling of solid–liquid fluidized beds of mono and binary particle mixtures. *Chemical Engineering Science*. 2009;64(16):3641-3658.
7. Khan MdS, Evans GM, Peng Z, et al. Expansion behaviour of a binary solid-liquid fluidised bed with different solid mass ratio. *Advanced Powder Technology*. 2017;28(12):3111-3129.
8. Khan MdS, Mitra S, Ghatage SV, Doroodchi E, Joshi JB, Evans GM. Segregation and dispersion studies in binary solid-liquid fluidised beds: A theoretical and computational study. *Powder Technology*. 2017;314(Supplement C):400-411.
9. Ayeni O, Tiwari SS, Wu C, Joshi JB, Nandakumar K. Behavior of particle swarms at low and moderate Reynolds numbers using computational fluid dynamics—Discrete element model. *Physics of Fluids*. 2020;32(7):073304.
10. Joshi JB, Nandakumar K. Computational Modeling of Multiphase Reactors. *Annual Review of Chemical and Biomolecular Engineering*. 2015;6(1):347-378.
11. Tiwari SS, Pal E, Bale S, et al. Flow past a single stationary sphere, 2. Regime mapping and effect of external disturbances. *Powder Technology*. 2019;365:215-243.
12. Bale S, Tiwari SS, Nandakumar K, Joshi JB. Effect of Schmidt number and D/d ratio on mass transfer through gas-solid and liquid-solid packed beds: Direct numerical simulations. *Powder Technology*. 2019;354:529-539.

13. Richardson J, Zaki W. Sedimentation and fluidization: part I. *Trans Inst Chem Eng.* 1954;32:35-53.
14. Hoffman RF, Lapidus L, Elgin JC. The mechanics of vertical moving fluidized systems: IV. Application to batch-fluidized systems with mixed particle sizes. *AIChE Journal.* 1960;6(2):321-324.
15. Epstein N, Pruden BB. Liquid fluidisation of binary particle mixtures—III Stratification by size and related topics. *Chemical Engineering Science.* 1999;54(3):401-415.
16. Wen C, Yu Y. A generalized method for predicting the minimum fluidization velocity. *AIChE Journal.* 1966;12(3):610-612.
17. Al-Dibouni MR, Garside J. Particle classification and intermixing in liquid fluidized bed. *Transactions of the Institute of Chemical Engineers.* 1979;57:94-103.
18. Galvin KP, Swann R, Ramirez WF. Segregation and dispersion of a binary system of particles in a fluidized bed. *AIChE Journal.* 2006;52(10):3401-3410.
19. Murli SV, Chavan PV, Joshi JB. Solid Dispersion Studies in Expanded Beds. *Ind Eng Chem Res.* 2007;46(6):1836-1842.
20. Chavan PV, Joshi JB. Analysis of Particle Segregation and Intermixing in Solid–Liquid Fluidized Beds. *Ind Eng Chem Res.* 2008;47(21):8458-8470.
21. Chen A, Grace JR, Epstein N, Lim CJ. Steady state dispersion of mono-size, binary and multi-size particles in a liquid fluidized bed classifier. *Chemical Engineering Science.* 2002;57(6):991-1002.
22. Clift R, Grace J, Weber M. *Bubbles, Drops, and Particles.* New York ; London : Academic Press; 1978. <https://trove.nla.gov.au/version/45620963>. Accessed April 20, 2018.
23. Gera D, Syamlal M, O'Brien TJ. Hydrodynamics of particle segregation in fluidized beds. *International Journal of Multiphase Flow.* 2004;30(4):419-428.
24. Gidaspow D. *Multiphase Flow and Fluidization: Continuum and Kinetic Theory Descriptions.* Academic Press; 1994.
25. Pandit AB, Joshi JB. Pressure drop in fixed, expanded and fluidized beds, packed columns and static mixers - A unified approach. *Reviews in Chemical Engineering.* 1998;14(4-5):321-371.
26. Jain V, Kalo L, Kumar D, Pant HJ, Upadhyay RK. Experimental and numerical investigation of liquid–solid binary fluidized beds: Radioactive particle tracking technique and dense discrete phase model simulations. *Particuology.* 2017;33:112-122.
27. Peng Z, Joshi JB, Moghtaderi B, Khan MdS, Evans GM, Doroodchi E. Segregation and dispersion of binary solids in liquid fluidised beds: A CFD-DEM study. *Chemical Engineering Science.* 2016;152(Supplement C):65-83.
28. Rahaman MdS, Choudhury MR, Ramamurthy AS, Mavinic DS, Ellis N, Taghipour F. CFD modeling of liquid-solid fluidized beds of polydisperse struvite crystals. *International Journal of Multiphase Flow.* 2018;99:48-61.
29. Syamlal M, O'Brien TJ. Simulation of granular layer inversion in liquid fluidized beds. *International Journal of Multiphase Flow.* 1988;14(4):473-481.
30. Molaei AE, Yu AB, Zhou ZY. Investigation of causes of layer inversion and prediction of inversion velocity in liquid fluidizations of binary particle mixtures. *Powder Technology.* 2019;342:418-432.
31. Di Renzo A, Cello F, Di Maio FP. Simulation of the layer inversion phenomenon in binary liquid--fluidized beds by DEM–CFD with a drag law for polydisperse systems. *Chemical Engineering Science.* 2011;66(13):2945-2958.
32. Rong LW, Dong KJ, Yu AB. Lattice-Boltzmann simulation of fluid flow through packed beds of spheres: Effect of particle size distribution. *Chemical Engineering Science.* 2014;116:508-523.

33. Kong B, Fox RO. A moment-based kinetic theory model for polydisperse gas–particle flows. *Powder Technology*. 2020;365:92-105.
34. Syamlal M, Rogers W, O'Brien TJ. *MFIX Documentation Theory Guide*. USDOE Morgantown Energy Technology Center, WV (United States); 1993.
35. Gidaspow D, Bezburuah R, Ding J. Hydrodynamics of circulating fluidized beds: Kinetic theory approach. In: *VII International Conference on Fluidization, Gold Coast (Australia), 3-8 May 1992*. Gold Coast (Australia): Illinois Inst. of Tech., Chicago, IL (United States). Dept. of Chemical Engineering; 1992. <https://digital.library.unt.edu/ark:/67531/metadc1100049/>. Accessed July 28, 2021.
36. Lun CKK, Savage SB, Jeffrey DJ, Chepurnyi N. Kinetic theories for granular flow: inelastic particles in Couette flow and slightly inelastic particles in a general flowfield. *Journal of Fluid Mechanics*. 1984;140:223-256.
37. Schaeffer DG. Instability in the evolution equations describing incompressible granular flow. *Journal of Differential Equations*. 1987;66(1):19-50.
38. Ding J, Gidaspow D. A bubbling fluidization model using kinetic theory of granular flow. *AIChE Journal*. 1990;36(4):523-538.
39. Syamlal M. The Particle-Particle Drag Term in a Multiparticle Model of Fluidization. *National Technical Information Service, Springfield, VA*. January 1987.
40. Bale S, Tiwari S, Sathe M, Berrouk AS, Nandakumar K, Joshi J. Direct numerical simulation study of end effects and D/d ratio on mass transfer in packed beds. *International Journal of Heat and Mass Transfer*. 2018;127:234-244.
41. Kalaga DV, Reddy RK, Joshi JB, Dalvi SV, Nandkumar K. Liquid phase axial mixing in solid–liquid circulating multistage fluidized bed: CFD modeling and RTD measurements. *Chemical engineering journal*. 2012; 191:475:490.
42. Ding Z, Tiwari SS, Tyagi M, Nandakumar K. Computational fluid dynamic simulations of regular bubble patterns in pulsed fluidized beds using a two-fluid model. *The Canadian Journal of Chemical Engineering*. 2021;n/a(n/a). doi:<https://doi.org/10.1002/cjce.24082>
43. Juma AKA, Richardson JF. Segregation and mixing in liquid fluidized beds. *Chemical Engineering Science*. 1983;38(6):955-967.
44. Zhang Y, Ran Z, Jin B, Zhang Y, Zhou C, Sher F. Simulation of Particle Mixing and Separation in Multi-Component Fluidized Bed Using Eulerian-Eulerian Method: A Review. *International Journal of Chemical Reactor Engineering*. 2019;17(11).
45. Peng C, Kong B, Zhou J, et al. Implementation of pseudo-turbulence closures in an Eulerian–Eulerian two-fluid model for non-isothermal gas–solid flow. *Chemical Engineering Science*. 2019;207:663-671.
46. Zhang C. sdfibm: a signed distance field based discrete forcing immersed boundary method in OpenFOAM. *Computer Physics Communications*. 2020;255:107370.
47. Kong B, Fox RO, Feng H, et al. Euler–euler anisotropic gaussian mesoscale simulation of homogeneous cluster-induced gas–particle turbulence. *AIChE Journal*. 2017;63(7):2630-2643.